Pergamon

Geochimica et Cosmochimica Acta, Vol. 66, No. 17, pp. 3055–3062, 2002

0016-7037/02 $22.00 + .00

PII S0016-7037(02)00893-1

Dissolution rates of minerals and their relation to surface morphology

ALEXANDER A. JESCHKE and WOLFGANG DREYBRODT*
Institute of Experimental Physics, University of Bremen, D-28334 Bremen, Germany

(*Received October* 11, 2001; *accepted in revised form February* 25, 2002)

Abstract—Experimentally observed dissolution rates of minerals in an aqueous solution are determined by surface reaction rates, mass transport by molecular diffusion through a diffusion boundary layer (DBL) and the morphology of the mineral's surface. By solving the transport equation in the presence of a diffusion boundary layer for surfaces containing open pores their contribution to the observed dissolution rates can be quantified. Furthermore dissolution rates are calculated for fractal surfaces. A general solution is given. Two extremes are discussed. If the surface controlled rate constant k is small compared to the mass transport constant $k_t = D/\varepsilon$ (ε thickness of DBL, D coefficient of diffusion), the rates are surface controlled and the entire surface contributes to the observed dissolution rate. In this case rates must be normalized to the B.E.T.-surface area. When $k \gg k_t$ the observed rates are limited by diffusion and information on k cannot be obtained. In intermediate cases a careful analysis is required. If ink bottle pores are present their contribution to the observed rates can be neglected and rates must be normalized to the geometrical envelope surface area, although in such cases the B.E.T.-surface area can be much larger. *Copyright © 2002 Elsevier Science Ltd*

1. INTRODUCTION

To measure reaction rates F of minerals in an aqueous solution one has to know the volume V of the solution and the surface area A of the mineral in contact with the solution. The free drift reaction in a closed system by mass balance causes a change of concentration c of the dissolved species by

$$V \cdot \frac{dc}{dt} = A \cdot k \cdot f(c_{eq}, c) = A \cdot F. \quad (1)$$

If solution rates F are measured at constant chemical composition the total amount F_t of the mineral released per time unit into the solution is measured. It is given by $F_t = A \cdot k \cdot f(c_{eq}, c)$. k is a mass transfer constant in units of cm s^{-1}, c_{eq} is the equilibrium concentration with respect to the mineral, and a general normalized rate law $f(c_{eq}, c)$ with $f(c_{eq}, 0) = 1$ is assumed. To determine the value of k the surface area A must be known. Mineral surfaces may be (a) flat and contain only steps and kinks, (b) they may contain pores and cracks, (c) they could be fractal, and (d) they contain deep pores connected by narrow channels to the surface (ink bottle pores). In all cases a geometric surface with surface area A_{geo} can be defined by an envelope to the real surface with surface area A_{real}. To characterize mineral surfaces a roughness factor $\xi = A_{real}/A_{geo}$ has been introduced [Anbeek (1992)]. In case (a) $\xi \lesssim 3$. In case (b) and (c) values of $\xi \geq 10$ may occur. If ink bottle pores are present values of ξ can be much larger [Hodson et al. (1997); Hodson (1998)]. Macropores (>50 nm) have been observed in naturally weathered feldspars, and mesopores and micropores (<50 nm) have been found in silicates after exposing them to dissolution [see Anbeek (1992) and references therein].

Most of the investigations on dissolution rate constants, especially those of silicates use the surface area, measured by the B.E.T. method on the scale of the absorbing species, e.g., N_2, Kr, Ar [see Gautier et al. (2001) and references therein]. Other studies on calcite [Plummer et al. (1978); Eisenlohr et al. (1999); Svensson and Dreybrodt (1992)] use geometrical surfaces. Comparison from data obtained by the rotating disk method from polished samples. [Liu and Dreybrodt (1997)] with those from batch experiments with broken particles confirm this choice [Svensson and Dreybrodt (1992)]. Also dissolution experiments on gypsum with the rotating disk method and batch experiments revealed that employing geometric surface areas is appropriate [Jeschke et al. (2001)].

There is a controversial debate whether B.E.T. areas or geometrical surface areas should be used. In most dissolution experiments one uses mineral grains with average sizes of 100 μm up to 1000 μm. If these are suspended in a solution, e.g., by vigorous stirring they are surrounded by a diffusion boundary layer (DBL) with thickness ε of about 10 μm, which separates the mineral surface from the turbulent bulk solution [Nielsen (1980); Jeschke et al. (2001)]. The ions detached from the surface of the mineral are transported through this layer by molecular diffusion with D, constant of diffusion. If the transport constant $k_t = D/\varepsilon$ is small compared to the reaction rate constant k the dissolution rates are controlled by molecular diffusion and the surface area A_{geo} defined by the enveloping inner border of the DBL determines the rates. On the other hand, if $k \ll k_t$ ions detached from the mineral are instantly transported into the bulk volume and the real surface of the particles determines the experimentally observed rates. A real surface is an idealized surface with an infinitely small resolution. B.E.T.-surface area measurements are performed by adsorption of molecules to this surface. The scale used to measure areas by this way is that of the molecule employed. Therefore B.E.T.-surface areas are regarded as a close approximation to the real surface area.

The flux of ions through the boundary layer from a flat part of the actual surface differs from that of a pore contained in it. Therefore measured rates are influenced by both, the diffusion boundary layer and the morphology of the surface; e.g. deep or shallow pores, fractal properties. For the interpretation of ex-

* Author to whom correspondence should be addressed (dreybrod@physik.uni-bremen.de).

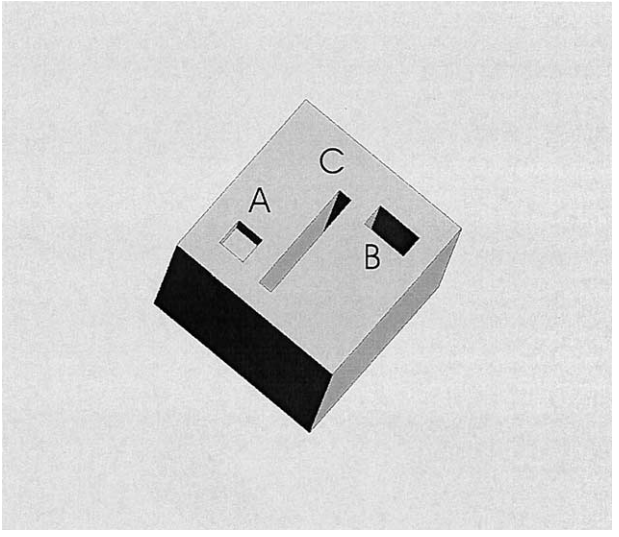

Fig. 1. Idealized surface of a mineral including several types of pores (A, B, C).

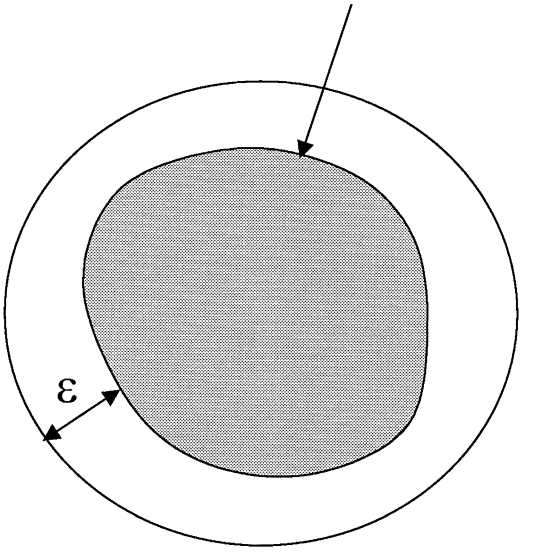

Fig. 2. Mineral particle, as used in batch experiments, surrounded by a diffusion boundary layer (DBL) with thickness ε. The arrow depicts the enveloping geometrical surface.

perimental data therefore both must be taken into account. This paper investigates theoretically rates normalized to the geometrical surface area for some idealized mineral surfaces, containing either open pores and cracks of microscales, mesoscales, or pores connected by small channels to the surface (ink bottle pores). Furthermore rates from fractal surfaces are discussed. As result we find that both surface morphology and mass transport through the boundary layer determine the rates.

2. THEORY

2.1. Idealization of the Problem

In general surfaces of mineral particles are not smooth. They exhibit steps, pores, and cracks. The dimensions of these, range from a few nm (micropores) to several 10 nm (mesopores) up to macropores of depth >50 nm. Figure 1 illustrates such an idealized surface. If the density of pores is high and the pores are deep, a large increase of the internal surface area compared to a completely flat surface is the outcome. B.E.T.-surface areas larger than a factor of 10 compared to the geometric surface area were observed on quartz particles of 80 μm diameter by Gautier et al. (2001). Here the geometric surface is obtained from the envelope of the rough surface by replacing the particles as spheres.

To estimate dissolution rates for particles with rough surfaces one must take into account the experimental conditions. In practically all experiments dissolution rates are not only determined by the surface reaction rate but also by diffusional transport of the detached ions away from the solid surface. In all experiments, where particles are kept in suspension, e.g., batch experiments with vigorous stirring, a particle is surrounded by a diffusion boundary layer as illustrated by Figure 2. This boundary layer around the geometrical surface is defined as the closest envelope to the rough surface of the mineral grain and extends to the distance ε, which can be estimated for small particles suspended in an aqueous, vigorously stirred, solution [Nielsen (1980), Zhang and Nancollas (1990)] by

$$\varepsilon = 5.74 \cdot \langle r \rangle^{0.145} (\Delta\rho)^{-0.285}\ (\mu\text{m}), \tag{2}$$

where $\langle r \rangle$ is the average radius of the particle in μm and $\Delta\rho$ is the density difference between the solid and the aqueous solution in g cm^{-3}. ε is the limiting value for solutions where enhancing stirring rates does not increase dissolution rates. ε shows only a slight dependence on $\langle r \rangle$. For $\Delta\rho = 2$ g cm^{-3} and $\langle r \rangle = 10$ μm one obtains $\varepsilon = 7$ μm, for $\langle r \rangle = 100$ μm one finds $\varepsilon = 9$ μm, and for $\langle r \rangle = 1000$ μm, $\varepsilon = 13$ μm. Such numbers have been confirmed experimentally on particles of rocksalt [Jeschke et al. (2001)]. For crushed particles with an irregular shape and a complex surface morphology the thickness of the DBL will vary and ε has to be considered as some average value. Although the concept of the DBL is highly idealized it can be reasonably well applied, as has been shown by Jeschke et al. (2001) by comparing the dissolution rates of gypsum obtained from rotating disk experiments and crushed particles in a batch experiment.

Dissolution rates at the surface may be complex functions of chemical composition of the solution at the surface, e.g., $CaCO_3$ [Plummer et al. (1978)]. Nevertheless, empirical rate equations can be found, which depend only on one representative species of the released ions [Lasaga (1998)], e.g.,

$$F(c_{\text{eq}}, c) = k_n \cdot \left(1 - \frac{c}{c_{\text{eq}}}\right)^n, \tag{3}$$

where n is some exponent. Such rate equations apply to gypsum, rocksalt, calcium carbonate, and quartz ($n = 1$). Close to saturation natural gypsum and calcium carbonate exhibit a change of the reaction order n [Eisenlohr et al. (1999); Jeschke et al. (2001)] to $n \approx 4$.

In our analysis we will restrict to linear rate equations with $n = 1$, because otherwise an analytical solution cannot be

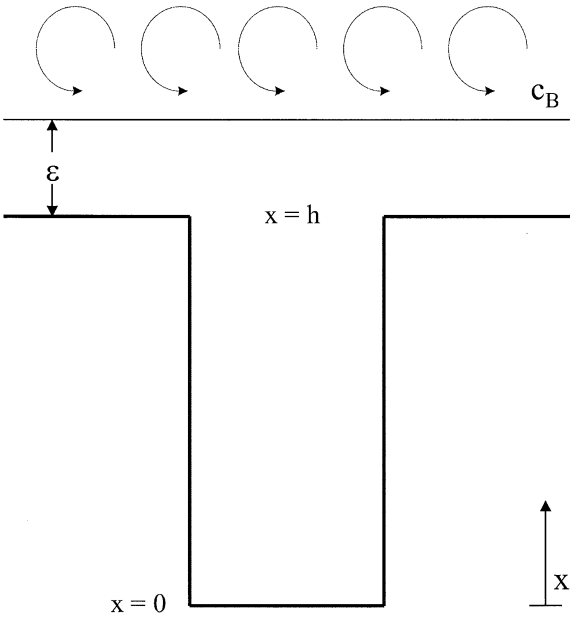

Fig. 3. Boundary conditions for dissolution in a pore of depth h.

obtained easily. In any case numerical solutions can be found. Inspection of the analytical solutions for linear dissolution, however, will provide insight into the qualitative behavior on the interplay of surface morphology, surface dissolution, and mass transport.

Since we restrict our analysis to one representative ion, the diffusion constant must be related to this ion. In a multicomponent solution an effective coefficient of diffusion must be used, which is some mean of the value of D_i for the individual species i in the solution [Lasaga (1998)].

2.2. Dissolution from Pores or Cracks

Figure 3 shows a pore of depth h. On its top the laminar diffusion boundary layer extends from $x = h$ to $x = h + \varepsilon$. At this position the concentration is given by c_B, the bulk concentration in the turbulent core of the bulk. At the surface and in the pore, dissolution takes place and the rates at the walls of the pore are given by

$$F = k(c_{eq} - c(x)), \tag{4}$$

where k is the surface controlled rate constant of the mineral, $c(x)$ is the concentration at position x, and c_{eq} its equilibrium concentration. By mass conservation one obtains [Gautier et al. (2001)]

$$A_B\left(-D\,\frac{\partial^2 c}{\partial x^2}\right) = Pk[c_{eq} - c(x)], \tag{5}$$

where A_B is the bottom surface area and P the corresponding perimeter of the pore. In this equation we assume that there are no gradients of concentration in direction perpendicular to x. This is true for the steady state, which is attained after the time $T \approx L^2/D$, where D is the constant of diffusion and L the characteristic dimension of the bottom area, e.g., its diameter [Luikov (1968)], provided the Biot criterion $\mathrm{Bi} = kL/D$ is sufficiently close to zero.

As an example, for the extreme case of rocksalt with $k = 5.10^{-2}$ cm s^{-1} [Alkattan et al. (1997)] for $L = 10^{-4}$ cm one finds $\mathrm{Bi} = 0.1$ and $T = 10$ s. This is sufficient time to obtain steady state in batch experiments. For materials with lower values of k, $\mathrm{Bi} < 0.1$ is valid for practically any experimental case. The solution of Eqn. 5 is given by

$$c(x) = C_1 \exp(-\alpha x) + C_2 \exp(+\alpha x) + c_{eq}, \tag{6}$$

$$\alpha = \sqrt{\frac{k}{D} \cdot \frac{P}{A_B}}.$$

The boundary condition for flux at the bottom, $x = 0$, is

$$-D\,\frac{\partial c(0)}{\partial x} = k[c_{eq} - c(0)]. \tag{7}$$

At $x = h$ the flux F from the pit must be equal to the flux through the boundary layer. Therefore,

$$F = -D\,\frac{\partial c(h)}{\partial x} = +\frac{D}{\varepsilon}\,[c(h) - c_B]. \tag{8}$$

By use of Eqs. 5–7 one finds the solution

$$c(x) = c_{eq} + \left(\frac{c_{eq} - c_B}{\varepsilon}\right) \cdot \frac{\left(\frac{k}{D} - \alpha\right)\exp(-\alpha x) - \left(\frac{k}{D} + \alpha\right)\exp(+\alpha x)}{\left(\frac{k}{D} - \alpha\right)\left(\alpha - \frac{1}{\varepsilon}\right)\exp(-\alpha x) + \left(\frac{k}{D} + \alpha\right)\left(\alpha + \frac{1}{\varepsilon}\right)\exp(+\alpha x)}. \tag{9}$$

The flux at $x = h$ into the diffusion boundary layer is equal to the flux into the bulk and is given by

$$F(h) = -D\,\frac{\partial c(x)}{\partial x}\bigg|_{x=h} = \frac{D}{\varepsilon}\,\alpha(c_{eq} - c_B) \cdot \frac{\left(\frac{k}{D} - \alpha\right)\exp(-\alpha h) + \left(\frac{k}{D} + \alpha\right)\exp(+\alpha h)}{\left(\frac{k}{D} - \alpha\right)\left(\alpha - \frac{1}{\varepsilon}\right)\exp(-\alpha h) + \left(\frac{k}{D} + \alpha\right)\left(\alpha + \frac{1}{\varepsilon}\right)\exp(+\alpha h)}. \tag{10}$$

Figure 4 depicts the concentration for two extreme cases. If the length $\lambda = 1/\alpha$ is small compared to the depth h of the pore the concentration is close to c_{eq} and only in the distance λ from the top of the pore it drops to some value smaller than c_{eq} (upper line). For the other case, where $\lambda \ll h$ one finds a behavior depicted by the lower curve. The curve shows a parabolic behavior and c_{eq} is nowhere attained in the pitch. When the depth h of the micropore is large with respect to λ, the flux from such a pore is found by taking $h \to \infty$ in Eqn. 10. As a result one finds

$$F = \frac{D\alpha[c_{eq} - c_B]}{\varepsilon\left(\alpha + \frac{1}{\varepsilon}\right)} = \frac{D[c_{eq} - c_B]}{\varepsilon + \lambda}. \tag{11}$$

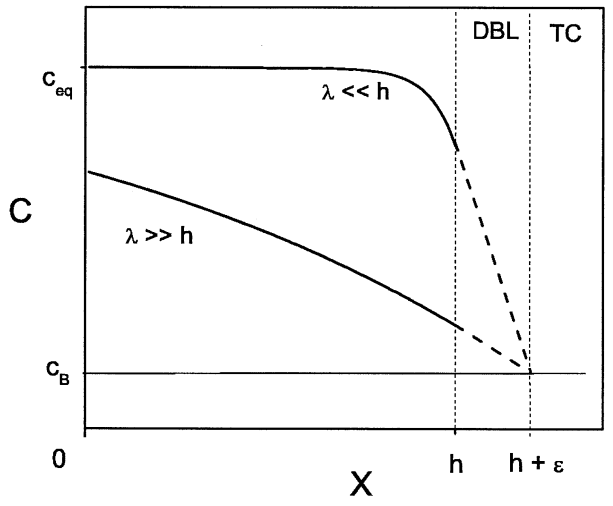

Fig. 4. Concentration profiles along the axis of a pore for $\lambda \ll h$ and $\lambda \gg h$ (see Eqn. 9). The region from h to $h + \varepsilon$ designates the diffusion boundary layer (DBL). The turbulent core (TC) with concentration c_B extends beyond $x = h + \varepsilon$.

One can see from this and the $c(x)$ profile in Fig. 4 that the flux is determined by an increase of the effective diffusion boundary layer by the distance λ. In most cases λ is small compared to ε, which was shown to be about 10 μm. Therefore for values of $\lambda \leq 1$ μm the flux from a deep pit with $h \approx 10\lambda$ is entirely controlled by diffusion.

The surface depicted in Figure 1 contains pores the cross section of which cover a part A_{pore} of the geometric surface area (i.e., $A_{\text{pore}} = \sum A_B$. The other part of the geometric surface area is covered by the flat surface area A_{flat}. This part can be regarded as pitches with depth $h = 0$. Calculating the limit of the flux from Eqn. 10 with $h \to 0$ one obtains for these parts of the particle.

$$F_{\text{flat}} = \frac{k\dfrac{D}{\varepsilon}}{k + \dfrac{D}{\varepsilon}}[c_{\text{eq}} - c_B]. \tag{12}$$

This is the well-known equation for mixed kinetics, where the transport coefficient of diffusion $k_t = D/\varepsilon$ and the surface controlled transfer constant k (cf. Eqn. 4) are of comparable magnitude [Dreybrodt (1988)]. The total rate observed in a batch experiment with particles obeying the conditions above is

$$F = \left[\frac{A_{\text{flat}}}{A_{\text{geo}}}\frac{D}{\varepsilon}\left(\frac{k}{k + \dfrac{D}{\varepsilon}}\right) + \frac{A_{\text{pore}}}{A_{\text{geo}}}\left(\frac{D}{\varepsilon + \lambda}\right)\right](c_{\text{eq}} - c_B). \tag{13}$$

For $k \gg D/\varepsilon$ and $\lambda \ll \varepsilon$ this reduces to

$$F = \frac{D}{\varepsilon}[c_{\text{eq}} - c_B] \tag{14}$$

and the dissolution rates are determined entirely by diffusion and the geometric surface area, no matter what the internal area of the pores contributes.

To explore the case where $h \ll \lambda$, one expands Eqn. 10 to first order in h to find

$$F_{\text{pore}} = \frac{k\dfrac{D}{\varepsilon}}{k + \dfrac{D}{\varepsilon}}(c_{\text{eq}} - c_B)\left\{1 + \frac{\left(\dfrac{\alpha^2 D^2}{k^2} - 1\right)}{\left(1 + \dfrac{D}{k\varepsilon}\right)} \cdot \frac{h}{\varepsilon}\right\}. \tag{15}$$

The term $\alpha^2 D^2/k^2$ can be reformulated by use of α^2 in Eqn. 6 as $D \cdot P/A_B \cdot k$; furthermore this term is large compared to 1 in all cases of interest, e.g., for pore sizes of 1 μm and $k \approx 10^{-2}$ cm s^{-1}, the extreme case of rocksalt, one obtains 10. Therefore one finds

$$F_{\text{pore}} = \frac{k\dfrac{D}{\varepsilon}}{k + \dfrac{D}{\varepsilon}}(c_{\text{eq}} - c_B)\left\{1 + \frac{\dfrac{Ph}{A_B}}{\left(1 + \dfrac{k\varepsilon}{D}\right)}\right\}. \tag{16}$$

Defining the surface area of a grain covered by pores as A_{pore} and that covered by the flat parts as A_{flat}, one gets

$$F = \frac{k\dfrac{D}{\varepsilon}}{\dfrac{D}{\varepsilon} + k}(c_{\text{eq}} - c_B)\left\{\frac{A_{\text{flat}}}{A_{\text{geo}}} + \frac{A_{\text{pore}}}{A_{\text{geo}}} \cdot \frac{\left(1 + \dfrac{Ph}{A_B}\right)}{\left(1 + \dfrac{k\varepsilon}{D}\right)}\right\}. \tag{17}$$

$(1 + Ph/A_B)$ represents the relation of the total internal surface area of a pore (zylindrical surface area + bottom surface area A_B) to its bottom surface area A_B. Therefore the internal surface contributes to the total dissolution rate F.

In the case $k \ll D/\varepsilon$ the total dissolution rate is enhanced by the factor $A_{\text{int}}/A_{\text{geo}}$, where A_{int} is the surface area measured on the scale of the smallest pores. In our idealized case this surface area is equal to the surface area measured by B.E.T. absorption.

As a consequence, where the reaction is determined by surface control, the B.E.T. surface area must be used.

In all considerations above we have assumed that the dissolution rate constants are identical everywhere. If one, however, assumes different rate constants; k_B at the bottom of the pore, k_w at the walls of the pore, and k_f at the flat parts, the situation becomes more complex. Recently, Gautier et al. (2001) have reported such a case. Employing dissolution experiments of quartz grains they have found the formation of etch pits, several μm deep with a diameter of about 0.1 μm on an otherwise flat surface. These pits contribute significantly to the B.E.T.-surface area which becomes up to 10 times larger than the geometric surface area. Nevertheless, in order to obtain reasonable rate constants the observed rates must be normalized to the geometric surface area. These rate constants still show a weak dependence on the B.E.T. surface as depicted by Figure 5. Gautier et al. (2001) interpret these data by using the following assumptions. Deep pits can form only if the dissolution rates at the bottom of the pit are higher by a factor of 12 than those in the flat parts, i.e., $k_B/k_f = 12$. Furthermore, they assume that rates at the wall of the pit are much smaller than that at its bottom, such that dissolution there does not contribute. From SEM photographs they find $A_{\text{pore}} \ll A_{\text{geo}} \approx A_{\text{flat}}$. For all rate constants as given by Gautier et al. (2001) $k \cdot \varepsilon/D \ll 1$ for $\varepsilon <$ 0.1 cm. Therefore, the rates are surface controlled and one obtains by modification of Eqns. 13–17,

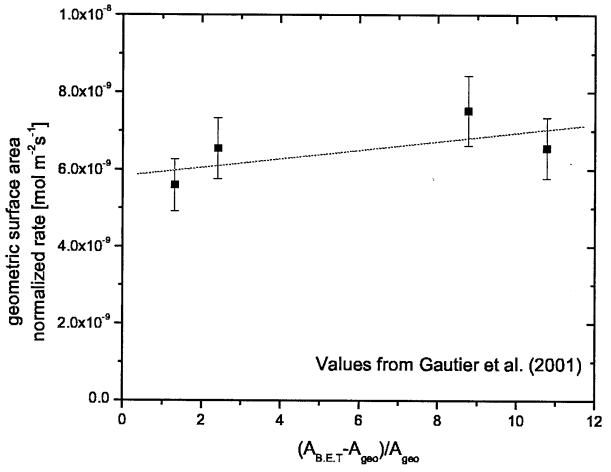

Fig. 5. Dependence of quartz dissolution rates normalized to geometric surface area on B.E.T.-surface area. The data points are taken from Gautier et al. (2001). The solid line represents Eqn. 19.

$$F = \frac{\left[k_f \cdot A_{\text{flat}} + k_B\left(1 + \frac{k_W}{k_B}\frac{Ph}{A_B}\right)\cdot A_{\text{pore}}\right]}{A_{\text{geo}}} \cdot (c_{\text{eq}} - c_B). \quad (18)$$

Using the Gautier et al. finding that $k_B A_{\text{pore}} \ll k_f A_{\text{flat}}$, and considering that $A_{\text{pore}}/A_{\text{geo}} = N$ is the total number of etch pits and therefore $P \cdot h \cdot N$ is the total wall surface of the pits on a grain, one finds

$$F = \frac{k_f(c_{\text{eq}} - c_B)\left[A_{\text{flat}} + \frac{k_W}{k_f} \cdot P \cdot h \cdot N\right]}{A_{\text{geo}}} = k_f(c_{\text{eq}} - c_B) \cdot \left[1 + \frac{A_{\text{B.E.T.}} - A_{\text{geo}}}{A_{\text{geo}}} \cdot \frac{k_W}{k_f}\right]. \quad (19)$$

This relation can be fitted to the experimental data using $k_W/k_f = 0.033$ and is presented by the full line in Fig. 5, whereby the values $A_{\text{B.E.T.}}$ and A_{geo} have been taken from Gautier et al. (2001).

2.3. Fractal Surfaces

So far the internal surface of pores has been assumed as flat. But one might as well assume that it also contains smaller pores, which again exhibit smaller pores and so on. A final limit will be reached at a scale, where the dimension of the smallest pores is in the order of a crystal unit cell.

This can be described by the concept of fractal surfaces [Mandelbrot (1983)]. To visualize such surfaces an example is shown by Figure 6. It depicts a face of a cubic pore with dimension a. This face is divided into 11×11 squares. On each of the shaded areas a new cubic pore is created. The surface area of this first generator is $\tilde{A}_1 = \frac{361}{121} a^2 = \frac{361}{121} \tilde{A}_0$. Repeating this procedure on each of the faces of the small squares in Fig. 6 produces a new surface $\tilde{A}_2$, with area $\tilde{A}_2 = \frac{361}{121} \tilde{A}_1$. After n repetitions we obtain a self-similar fractal surface with area $\tilde{A}_n = (\frac{361}{121})^n \tilde{A}_0 = (f)^n A_0$, where f is the surface multiplication factor in each single step.

If we start as an example with $a = 1$ μm and repeat this procedure down to a scale of a crystal unit cell, i.e., 1 nm we need three iterations and the total internal surface area becomes larger by a factor of 27. Since the B.E.T.-method measures surface areas on the scale of the molecules used for adsorption the B.E.T. surface will be close to this surface area.

To find the dissolution rates, one might start with the smallest scale pore, which is depicted in Figure 7. For each of those pores one assumes a rate law given by Eqn. 4. To investigate the flux out of each of the smallest pores, the following boundary conditions must be considered. At stationary state a fixed concentration c_i is achieved at the top of each pore, where i designates pore i. Furthermore, there is no diffusion boundary layer, i.e., $\varepsilon = 0$. In practically all cases of interest (natural minerals) one finds that the depths of pores $h \ll \lambda$. Therefore Eqn. 17 can be used in the limit of $\varepsilon \to 0$ to estimate the average flux into the next larger pore. It is given by

$$F_0 = k(c_{\text{eq}} - c) \cdot f, \quad (20)$$

where f is the surface multiplication factor. The boundary condition for the next larger pore is given by Eqn. 7, where k has to be replaced approximately by an average value $f \cdot k$. By repeating this procedure to the next larger pore we find

$$F_2 = k(c_{\text{eq}} - c) \cdot f^2 \quad (21)$$

and after n repetitions until the largest pore is reached we find

$$F_n = k(c_{\text{eq}} - c) \cdot f^n \quad (22)$$

as flux into this pore. The flux out of this pore into the bulk across the boundary layer is finally given by use of Eqn. 17 and replacing k by $f^n \cdot k$,

$$F = \frac{f^n k}{\frac{f^n k \varepsilon}{D} + 1}(c_{\text{eq}} - c_B)\left\{\frac{A_{\text{flat}}}{A_{\text{geo}}} + \frac{A_{\text{pore}}}{A_{\text{geo}}} \cdot \frac{\left(1 + \frac{Ph}{A_B}\right)}{\left(1 + \frac{f^n k \varepsilon}{D}\right)}\right\}. \quad (23)$$

If $f^n k\varepsilon/D \ll 1$ the reaction is surface controlled and k can be determined by estimating $f^n \approx A_{\text{B.E.T.}}/A_{\text{geo}}$. On the other hand, if $f^n k\varepsilon/D \gg 1$ the reaction becomes diffusion limited and a determination of surface rates is not possible.

2.4. Porous Surfaces and Ink Bottle Pores

Additional surface area can result from naturally occuring pores within the mineral, which become open to the surface by grinding or breaking the material [Hodson (1998)]. An idealized form of such an ink bottle pore connected to the surface by a smaller channel is depicted in Figure 8. We assume that at steady state the concentration in the pore does not show significant gradients and is given by c_p. Therefore the boundary conditions for the concentration in the channel are $c(0) = c_p$ at $x = 0$, and otherwise are given by Eqn. 8 at $x = h$, its exit to the solution. Using these conditions one finds for the flux F into the solution at $x = h$,

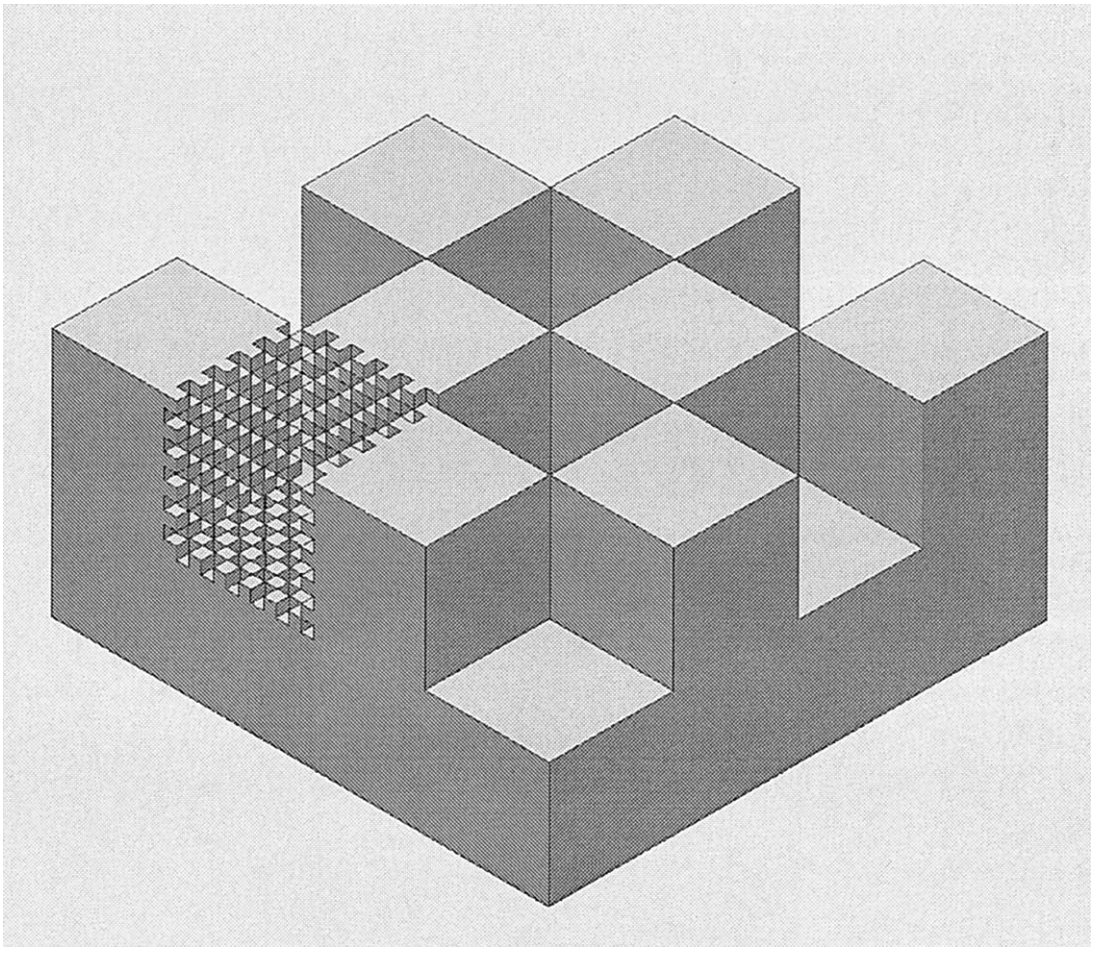

Fig. 6. Visualization of a fractal surface. The large scale cubes depict the biggest pores on the mineral's surface. Each of those shows the structure depicted in the left-hand side pore. This procedure is repeated to the scale of the lattice cells of the mineral.

$$F = \left(\frac{D\alpha}{\varepsilon}\right) \cdot \frac{\{2(c_p - c_{eq}) + (c_{eq} - c_B)[\exp(-\alpha h) + \exp(+\alpha h)]\}}{\left(\alpha - \frac{1}{\varepsilon}\right)\exp(-\alpha h) + \left(\alpha + \frac{1}{\varepsilon}\right)\exp(+\alpha h)}. \quad (24)$$

Again two limits can be considered.
If $\lambda \ll h$, one obtains

$$F = \frac{D}{\varepsilon + \lambda}(c_p - c_B). \quad (25)$$

F is completely contolled by diffusion. On the other hand, for $\alpha h \ll 1$ one finds

$$F = \frac{D}{\varepsilon}\frac{(c_p - c_B)}{1 + \frac{h}{\varepsilon}}. \quad (26)$$

The unknown value of c_p is obtained by mass balance. The total amount of mineral dissolved at c_p in the pore must be equal to the amount transported through the channel. One thus obtains

$$c_p = \frac{k_D c_B + k c_{eq}\frac{A_p}{A_m}}{k_D + k\frac{A_p}{A_m}}, \quad (27)$$

k_D is the diffusional transport coefficient, either $D/(\varepsilon + \lambda)$; Eqn. 25, or $(D/\varepsilon)\ [1 - (h/\varepsilon)] \approx D/\varepsilon$ (Eqn. 26). A_p is the internal surface area of the pore and A_m is the cross sectional area of the channel connecting the pore to the solution. The observed rate for a particle with such a porous surface is given by

$$F = \left[\frac{A_{flat}}{A_{geo}} \cdot \frac{D}{\varepsilon}\left(\frac{k}{k + \frac{D}{\varepsilon}}\right)(c_{eq} - c_B) + \frac{A_{ink}}{A_{geo}} \cdot \frac{D}{\varepsilon + \lambda}(c_p - c_B)\right]. \quad (28)$$

Here A_{ink} is the sum of all channel cross sections A_m. If $A_{ink} \ll A_{flat}$ or $k \gg D/\varepsilon$ the rate F is mainly determined by surface controlled dissolution from the geometric surface, although the B.E.T. surface might be much larger.

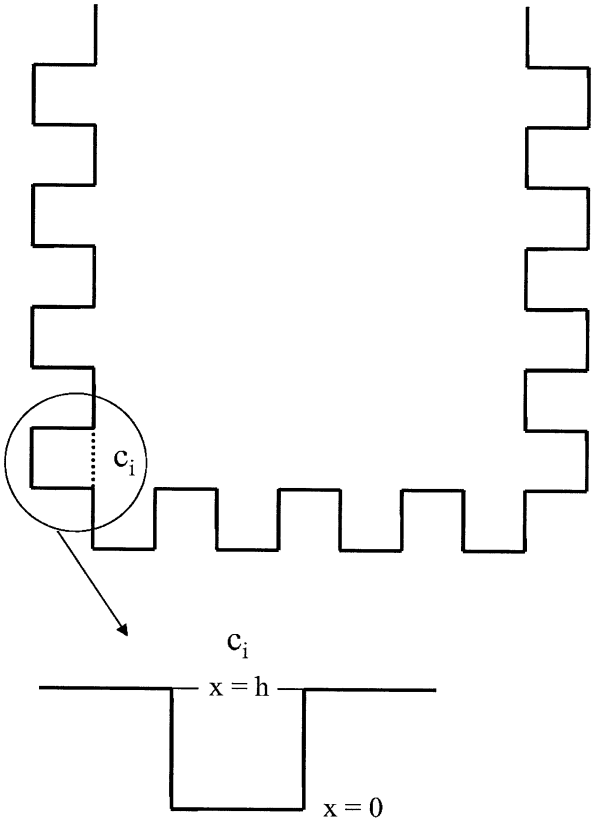

Fig. 7. Pores on the smallest scale embedded into a pore of the next higher scale. The concentration at the exit of pore i is c_i.

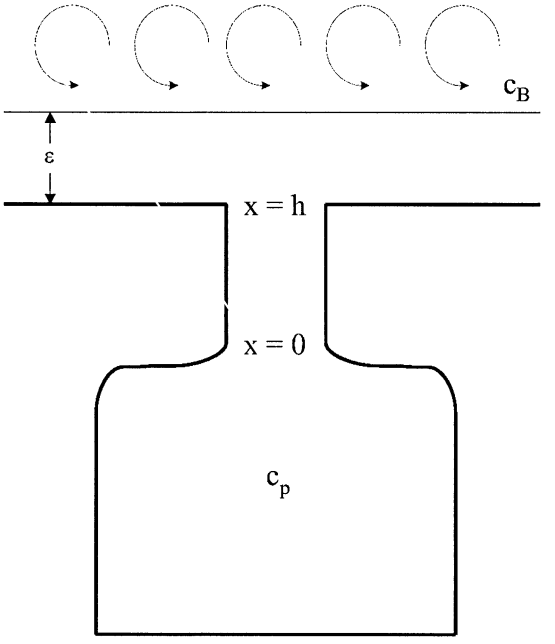

Fig. 8. Ink bottle pore connected by a channel to the solution. The concentration c_p in the pore is assumed as constant.

3. DISCUSSION AND CONCLUSION

To judge the consequences of the rate equations derived in this work for specific experiments knowledge of the values of ε, k, and pore depth h is necessary. For most minerals of geological relevance the ratio is $\lambda/h \gg 1$ for pore sizes below 1 μm. As an example; k is in the order of 10^{-4} to 10^{-5} cm s^{-1} for limestone [Buhmann and Dreybrodt (1985)]. Therefore $\lambda/h = 16$ for $h = 1$ μm and $\lambda/h = 160$ for $h = 0.01$ μm. For quartz the value of $k \approx 10^{-7}$ cm s^{-1} and one finds $\lambda/h = 500$ for $h = 1$ μm [Gautier et al. (2001)]. Silicates exhibit similar or even smaller values of k. For gypsum $k = 7 \times 10^{-3}$ cm s^{-1} [Jeschke et al. (2001)] and $\lambda/h = 1.6$ for $h = 1$ μm, but 16 for $h = 0.01$ μm. Therefore for pores sizes below 1 μm the total surface of the pore contributes to the dissolution, see Eqn. 17. This is also true for fractal pores (see Eqn. 23). Two cases must then be considered, see Eqn. 17 and Eqn. 23: (a) If $k \ll D/\varepsilon$ the entire flux through the geometric area is surface controlled and one obtains the correct value of k by use of the B.E.T.-surface. (b) If $k \gg D/\varepsilon$, the reaction is diffusion limited and the contribution from pores becomes supressed. In this case information on k cannot be obtained.

If ink bottle pores determine B.E.T. surface areas, as may be seen from hysteresis of the absorption isotherms, Eqn. 28 is valid and the geometrical surface area must be used to determine k when rates are surface controlled.

To obtain a reasonable estimation of reaction rate constants one has to take into account as much information as possible on the morphology of the surface. On the other hand, for minerals with low values of k the results will not depend critically on the thickness ε of the diffusion boundary layer and no detailed information on this is needed in standard experiments. In this work only extreme cases have been discussed. Intermediate cases, not discussed here, can be derived from Eqn. 10.

For minerals with sufficiently high dissolution rates, e.g., calcite, gypsum, comparison of results from batch experiments using crushed particles, and rotating disk experiments using polished mineral surfaces with much smaller geometrical surface can be helpful. If in such experiments use of the geometric surface areas leads to consistent values of k one can conclude that the real surface area is close to the B.E.T.-surface area as is the case in limestone. For quartz and silicate minerals, owing to the low rates, this is not possible. In conclusion, it has been shown that experimentally observed dissolution rates should be interpreted taking into account the following: as much detailed knowledge as possible on the surface morphology, and also knowledge of transport properties due to molecular diffusion in the specific experiment.

Acknowledgments—One of us, A. J. thanks the "Stiftung Constantia v.1823, Bremen" for financial support. We thank Dr. Sverjensky for helpful suggestions.

Associate editor: D. A. Sverjensky

LIST OF SYMBOLS

a	cubic pore dimension (cm)
α	abbreviation for $\sqrt{k \cdot P/DA_B}$
A	surface area (cm^2)
A_B	bottom surface area of a pit (cm^2)
$A_{B.E.T.}$	surface area measured by B.E.T. (cm^2)
A_{flat}	flat surface area (cm^2)
A_{geo}	geometric surface area (cm^2)
A_{ink}	ΣA_m (cm^2)
A_{int}	surface area in the scale of the smallest pore (cm^2)
A_m	cross sectional area of an inkbottle pore at the bottleneck (cm^2)
$\tilde{A}_n$	fractal surface area after n steps (cm^2)
A_p	internal surface area of an inkbottle pore (cm^2)
A_{pore}	area of A_{geo} which is covered by pores (pore bottom area) (cm^2)
A_{real}	real surface area (cm^2)
Bi	Biot criterion
c	concentration (mol cm^{-3})
c_B	bulk concentration (mol cm^{-3})
c_{eq}	equilibrium concentration (mol cm^{-3})
c_p	concentration in an inkbottle pore (mol cm^{-3})
D	coefficient of diffusion ($cm^2\ s^{-1}$)
ε	thickness of the diffusion boundary layer (DBL) (cm)
f	fractal surface multiplication factor for one step
F	flux (mol $cm^{-2}\ s^{-1}$)
F_{flat}	flux from A_{flat} (mol $cm^{-2}\ s^{-1}$)
F_{pore}	flux out of a pore (mol $cm^{-2}\ s^{-1}$)
F_t	total amount of the mineral per time unit
h	pore depth (cm)
k	surface rate constant (cm s^{-1})
k_f	rate constant of the flat parts (cm s^{-1})
k_t	mass transport constant (cm s^{-1})
k_B	rate constant of the bottom of a pore (cm s^{-1})
k_W	rate constant of the walls of a pore (cm s^{-1})
L	characteristic dimension (cm)
λ	$1/\alpha$ length of exponential decay (cm)
n	reaction order
N	total number of pores
P	pore perimeter (cm)
$\langle r \rangle$	average particle radius (μm)
ρ	density (g cm^{-3})
t	time (s)
T	time constant (s)
V	volume (cm^3)
x	coordinate (cm)
ξ	roughness factor

REFERENCES

Alkattan M., Oelkers E. H., Dandurand J. L., and Schott J. (1997) Experimental studies of halite dissolution kinetics. 1. The effect of saturation state and the presence of trace metals. *Chem. Geol.* **137,** 201–219.

Anbeek C. (1992) Surface roughness of minerals and implications for dissolution studies. *Geochim. Cosmochim. Acta* **56,** 1461–1469.

Buhmann D. and Dreybrodt W. (1985) The kinetics of calcite dissolution and precipitation in geologically relevant situations of karst areas. 1. Open system. *Chem. Geol.* **48,** 189–211.

Dreybrodt W. (1988) *Processes in Karst Systems*. Springer Series in Physical Environment No. 4. Springer-Verlag.

Eisenlohr L., Meteva K., Gabrovšek F., and Dreybrodt W. (1999) The inhibiting action of intrinsic impurities in natural calcium carbonate minerals to their dissolution kinetics in aqueous H_2O–CO_2 solutions. *Geochim. Cosmochim. Acta* **63,** 989–1002.

Gautier J. M., Oelkers E. H., and Schott J. (2001) Are quartz dissolution rates proportional to B.E.T. surface areas? *Geochim. Cosmochim. Acta* **65,** 1059–1070.

Hodson M. E. (1998) Micropore surface area variation with grain size in unweathered alkali feldspars: implications for surface roughness and dissolution studies. *Geochim. Cosmochim. Acta* **62,** 3429–3435.

Hodson M. E., Lee M. R., and Parsons I. (1997) Origins of the surface roughness of unweathered alkali feldspar grains. *Geochim. Cosmochim. Acta* **61,** 3885–3896.

Jeschke A. A., Vosbeck K., and Dreybrodt W. (2001) Surface controlled dissolution rates of gypsum in aqueous solutions exhibit nonlinear dissolution kinetics. *Geochim. Cosmochim. Acta* **65,** 27–34.

Lasaga A. C. (1998) *Kinetic Theory in Earth Sciences.* Princeton Series in Geochemistry. Princeton University Press.

Liu Z. and Dreybrodt W. (1997) Dissolution kinetics of calcium carbonate minerals in H_2O–CO_2 solutions in turbulent flow: The role of the diffusion boundary layer and the slow reaction $H_2O + CO_2 \rightarrow H^+ + HCO_3^-$. *Geochim. Cosmochim. Acta* **61,** 2879–2889.

Luikov A. V. (1968) *Analytical Heat Diffusion Theory*. Academic.

Mandelbrot B. B. (1983) *The Fractal Geometry of Nature*. Freeman.

Nielsen A. E. (1980) Transport control in crystal growth from solution. *Croatica Chem. Acta* **53,** 255–279.

Plummer L. N., Wigley T. M. L., and Parkhurst D. L. (1978) The kinetics of calcite dissolution in CO_2–water systems at 5° to 60 °C and 0.0 to 1.0 atm CO_2. *Am. J. Sci.* **278,** 179–216.

Svensson U. and Dreybrodt W. (1992) Dissolution kinetics of natural calcite minerals in CO_2–water systems approaching calcite equillibrium. *Chem. Geol.* **100,** 129–145.

Zhang J. W. and Nancollas G. H. (1990) Mechanisms of growth and dissolution of sparingly soluble salts. In *Mineral-Water Interface Geochemistry* (eds. M. F. Hochella and A. F. White), pp. 365–396. Mineralogical Society of America.